# A framework for MR phase reconstruction from multi-channel RF coils

Joseph Dagher[1], Kambiz Nael[2], Arthur Gmitro[3], and Ali Bilgin[4]

[1]*Medical Imaging, Electrical and Computer Engineering, University of Arizona, Tucson, AZ, United States,* [2]*Medical Imaging, University of Arizona, Arizona, United States,* [3]*Medical Imaging, Optical Sciences, University of Arizona, Arizona, United States,* [4]*Biomedical Engineering, Electrical and Computer Engineering, University of Arizona, Arizona, United States*

The purpose of this study is to improve the precision and robustness of MR phase images when acquired using an array of receive coils (channels). Combining phase images from multiple channels is a difficult problem hindered by challenges such as phase wrapping, noise and the unknown phase offset between each of the channels[1,4]. We present here a method which reconstructs the underlying object's phase image (i.e., tissue phase), as well as the channels' phase offsets, from a single Multi-Echo Gradient Echo (MEGE) scan, without requiring a reference scan[4]. **Methods**: The proposed phase estimator is described using the block diagram in Figure 1. In the first pass, raw measurements from all echoes **t** and all channels **c**, $\mathbf{m}_{\{t,c\}}$, are combined into a single phase image using consistency-check formalism. Specifically, in this formalism (1), the phase in each voxel is chosen such that, for all channels, the linear phase build-up between echo pairs (TE1,TE2) and (TE1,TE3) is maximally "consistent" (in an L2-sense). Since this minimization step is performed one voxel at a time, rapid brute force 1-D search methods could be used to find the appropriate solution. Note that this step estimates the *linear* component in the phase build-up that most accurately explains the data across echoes. Any remaining phase ($\phi^{\mathbf{rem}}_{\{\mathbf{t,c}\}}$) is explained by factors such as noise, channel-dependent phase offset ($\phi^{\mathbf{0}}_{\mathbf{c}}$), and any non-linear phase component. In the second pass, the estimator extracts phase offsets from $\phi^{\mathbf{rem}}_{\{\mathbf{t,c}\}}$ simply by assuming that the low-spatial frequencies of $\phi^{\mathbf{rem}}_{\{\mathbf{t,c}\}}$ are mostly attributed to $\phi^{\mathbf{0}}_{\mathbf{c}}$, (2)-(3). In the final pass, we "refine" the phase estimate of the first pass by using temporal regularization (4). This is achieved by first removing the offset estimate obtained in pass 2, and then finding the linear phase signal (across echo time) which minimizes the norm of any remaining phase signal. Ignoring any non-linear phase variations across time, this remaining signal is solely attributable to noise. Similar to the first pass, this minimization is performed voxel-by-voxel, and thus could be rapidly performed using brute-force search methods. We make an important observation here: the minimization metric (1) of the first pass would normally have multiple solutions, due to ambiguities from both phase wrapping and noise. Such ambiguities in phase have been quantified in closed-form in our earlier work (Phase Ambiguity Function, PAF)[1]. There, we showed that an optimal choice of 3 echo times results in minimum overlap between PAFs, and thus maximum information about the original phase's value. In this work, we use the MAGPI optimizer described in [1] to design echo times that guarantee no overall ambiguity from phase wrapping (despite using long echo time spacing), and minimal ambiguity from noise. We tune the MAGPI optimizer according to the constraints of the sequence of interest (minimum echo time, minimum echo spacing, bandwidth, etc.). The resulting 3 echoes (8.13, 15.15, 24.53 ms) guarantee an RMS error of 1.8Hz over a dynamic range of phase values between [-200,200] Hz. This implies that the search method in the third pass (4) needs only to explore a neighborhood defined by the expected error in the first phase estimate ($\phi^{\mathbf{cc}}\pm$1.8Hz). Finally, we note that reconstructing 1 voxel with our method requires ~ 1.3ms on a personal computer with MATLAB.

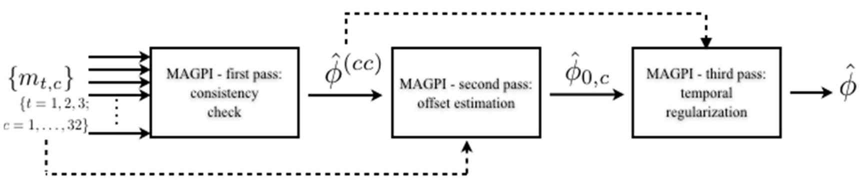


**Figure 1 –** Block diagram of the proposed MAGPI phase estimator

$$\hat{\phi}^{(cc)} = \arg\min_{\phi_t} \sum_{k=2,3} \sum_{c} ||m_{1,c} e^{i2\pi\phi_t(\mathrm{TE}(1)-\mathrm{TE}(k))} - m_{k,c}||^2 \tag{1}$$

$$|m_{k,c}| \exp(-i\phi^{rem}_{k,c}) = m_{k,c} e^{i2\pi\hat{\phi}^{(cc)}\mathrm{TE}(k)} \tag{2}$$

$$\exp(-i\phi^0_c) \approx \mathrm{LPF}\left\{\sum_k |m_{k,c}| \exp(i\phi^{rem}_{k,c})\right\} \tag{3}$$

$$\hat{\phi} = \arg\min_{\phi_t} \sum_{k=1}^{3} \sum_{c} ||m_{k,c} e^{i\phi^0_c} e^{i2\pi\phi_t \mathrm{TE}(k)} - ||m_{k,c}|| \,||^2 \tag{4}$$

We compare phase images reconstructed with our technique using a MEGE scan to Siemens product phase images reconstructed from a GRE acquisition on a 3T Skyra. The common parameters for both scans were the following: 3D FOV 256x192mm with 64 slices, flow compensation along read-out, matrix size 512x384, yielding a voxel size of 0.5x0.5x2mm, TR=31ms, BW=330Hz/pxl. The MEGE MAGPI echoes were at 8.13, 15.15 and 24.53ms. The GRE echo was at 25ms. We emphasize that the MAGPI MEGE scan takes as long as acquiring one GRE. **Results**: Figure 2 illustrates the resulting phase images, shown with different levels of high-pass filtering in order to display tissue variations of interest. Table 1 lists the Contrast to Noise Ratio (CNR) as computed around cortical and venous regions in various slices. We list 2 CNRs for each ROI/method, each corresponding to the CNR obtained with homodyne[2] (Fig 2a-b) and bilateral[3] (Fig. 2c-d) filters, respectively. **Discussion:** We note the gain in the quality and robustness of phase images as obtained with MAGPI. In addition to a clear improvement in visual quality, particularly at small phase values, we also observe gains in CNR with factors as high as 8 in some ROIs. The average gain in CNR obtained with MAGPI over all ROIs was around a factor of 4. We also note the performance of the commonly-used homodyne filter which suffers from blooming artifacts in regions with large contrast variations (e.g., cortical regions around the boundary). The bilateral filter, applied directly in phase domain, resolves these artifact issues[3] at the expense of a reduction in CNR. This contrast reduction is particularly seen with the dicom phase (Fig 2d) where large noise (low CNR) reduces the bilateral filter's edge preservation capacity and "amplifies" its de-noising component. MAGPI phase, however, is particularly well-suited to bilateral filtering where edge information is enhanced without artifacts and noise amplification.

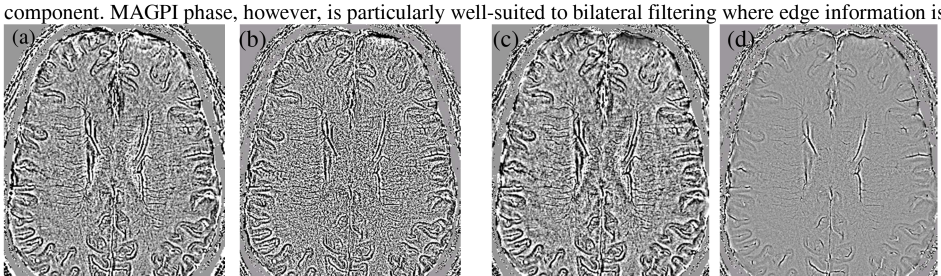


**Figure 2 –** High pass filtered phase, ***displayed between ±0.5Hz***. In (a)-(b) images are high pass filtered using the "homodyne" filter[2] while in (c)-(d) images are high pass filtered using the bilateral filter[3]. In (a)-(c) the filters operate on the phase obtained with the MAGPI estimator, while in (b)-(d) the filters operate on product images from the scanner. The commonly acquired phase (b) is noisier here due to our higher (more rapid) readout bandwidth. The channel offsets are not shown, due to space limitations.

Table 1 – CNR in different ROIs/slices – **ROIs were picked around cortical boundaries, similar to [3]**

| | **ROI-1** | | **ROI-2** | | **ROI-3** | | **ROI-4** | | **ROI-5** | | **ROI-6** | | **ROI-7** | |
|---|---|---|---|---|---|---|---|---|---|---|---|---|---|---|
| **MAGPI** (homodyne \| bilateral) | 2.77 | 3.75 | 3.74 | 2.67 | 2.62 | 2.64 | 3.26 | 2.72 | 2.73 | 2.60 | 1.1 | 1.25 | 3.84 | 2.37 |
| **Dicoms** (homodyne \| bilateral) | 0.37 | 0.51 | 1.54 | 1.06 | 1.24 | 0.91 | 2.01 | 1.45 | 0.6 | 0.63 | 0.2 | 0.15 | 1.37 | 0.79 |

**References: [1]** Dagher J, Reese T, Bilgin A, MRM 2013, early view (10.1002/mrm.24636). **[2]** Haacke EM, Xu Y, Cheng YC, Reichenbach JR, MRM 2004; 52:612-618. [**3**] McPhee KC, Denk C, Al-Rekabi Z, Rauscher A, MRM 2011; 29:1023-1029. **[4]** Robinson S. *et. al.*, MRM 2011; 65:1638-1648.